Vehicle Lateral Stability Management Using Gain-Scheduled Robust Control

Seung-Han You*, Joon-Sang Jo, Seungjin Yoo
School of Mechanical and Aerospace Engineering, Seoul National University, San 56-1, Sillim-dong, Gwanak-gu, Seoul 151-742, Korea
Jin-Oh Hahn
Department of Mechanical Engineering, Massachusetts Institute of Technology, Cambridge, MA 02139, USA
Kyo Il Lee
School of Mechanical and Aerospace Engineering, Seoul National University, San 56-1, Sillim-dong, Gwanak-gu, Seoul 151-742, Korea

This paper deals with the design of a yaw rate controller based on gain-scheduled H_∞ optimal control, which is intended to maintain the lateral stability of a vehicle. Uncertain factors such as vehicle mass and cornering stiffness in the vehicle yaw rate dynamics naturally call for the robustness of the feedback controller and thus H_∞ optimization technique is applied to synthesize a controller with guaranteed robust stability and performance against the model uncertainty. In the implementation stage, the feed-forward yaw moment by driver's steer input is estimated by the disturbance observer in order to determine the accurate compensatory moment. Finally, HILS results indicate that the proposed yaw rate controller can satisfactorily improve the lateral stability of an automobile.

Key Words : Vehicle Stability Management, Yaw Rate Control, H_∞ Control, Robust Performance, Gain Scheduling, Disturbance Observer, Brake Force Distribution

1. Introduction

Today, there is greater demand for active safety system to prevent accidents through artificial intervention. This system extends beyond the passive safety notion of merely minimizing damage from accidents and it is increasingly becoming recognized in the market as a necessity rather than a luxury option (Langwieder et al., 2003 ; Rieth and Schwarz, 2004). Following this trend, extensive research has been carried out on a variety of driver-subsidiary, active vehicle control methods to prevent vehicles from unstable longitudinal and/or lateral slip. The following approaches, although not an exclusive list, summarize recent achievements : electronic stability control (ESC), vehicle dynamics control (VDC), direct yaw moment control (DYC), vehicle stability control (VSC), vehicle stability assist (VSA) and vehicle stability management (VSM) (Pilutti et al., 1998 ; Zanten et al., 1998 ; Tseng et al., 1999 ; Yasui et al., 1996 ; Nishimaki et al., 1999). These systems are all based on almost the similar physical principles but are merely named differently by the developing companies. Among them, the term VSM (Vehicle Stability Management) is used in this paper. Although there have been other alternative candidates relating to actively

* Corresponding Author,
E-mail : shyoul@gmail.com
TEL : +82-2-880-7143; **FAX** : +82-2-883-1513
School of Mechanical and Aerospace Engineering, Seoul National University, San 56-1, Sillim-dong, Gwanak-gu, Seoul 151-742, Korea. (Manuscript **Received** April 4, 2006; **Revised** August 18, 2006)

securing vehicle stability such as 4WS (Four Wheel Steer), AFS (Active Front wheel Steer) and differential traction, the recent main stream of active vehicle safety system is focused on braking intervention by differential braking. This appears to be mainly due to the hardware reliability and cost efficiency resulting from the existing technical outcome relating to ABS (Anti-lock Brake System) and TCS (Traction Control System), which hold wheel slip in the linear slip region during braking/acceleration.

Since vehicle tire has the characteristic nature that its friction force is saturated or diminishes past a tire grip limit, tire friction force hardly ever returns to a stable linear friction region of itself without proper artificial interventions once it enters the nonlinear region. Consequently, the excessive tire slips such as 1) wheel spinning or wheel locking in the longitudinal motion, 2) drift out (understeer) or spin out (oversteer) in the lateral motion are most likely to occur when a tire force becomes saturated. Therefore, the key role of a vehicle stability management system is to keep tire lateral force of the front and/or rear wheels from exceeding the grip limit by the compensatory yaw moment through differential braking. Specifically, vehicle stability management system suppresses the lateral slip of the front (/rear) wheels by generating the compensatory pressure at the inner (/outer) wheels when understeer (/oversteer) cornering motion occurs as a result of excessive lateral slip in the front (/rear) wheels.

Among the various subsystems of a vehicle stability management system, such as stability analysis, control intervention criterion, parameter/state estimation, hydraulic actuator control and vehicle motion control, this paper mainly focuses on the vehicle motion control part that analytically determines how much compensatory yaw moment is needed to restore vehicle lateral stability, and then appropriately distributes the designed control yaw moment to the braking force in each wheel.

This paper presents a new yaw-rate-control-based vehicle stability management strategy with the robustness against the model uncertainties, such as un-modeled dynamics and vehicle parametric uncertainties. The designed yaw rate controller is intended to reduce body sideslip, prevent vehicle rollover, as well as allow the controlled vehicle to track the reference yaw rate. Uncertain factors such as vehicle mass and cornering stiffness in the vehicle yaw rate dynamics require the feedback controller to be robust and thus H_∞ optimization technique is applied to synthesize a controller with guaranteed robust stability and performance against the model uncertainty. In the implementation stage, the disturbance observer is employed to determine the accurate compensating yaw moment, which should be assigned to differential braking. The braking force at the individual wheels for generating artificial yaw moment is distributed according to the braking/releasing efficiency order of the individual wheels and intervention priority, which are based on the interaction between lateral tire force and longitudinal tire force. The HILS results conducted in the various driving conditions reveal that the proposed vehicle stability management system can improve the lateral stability of a vehicle to a satisfactory level.

2. Vehicle Model

The essential features of the vehicle lateral or steering dynamics can be effectively described by the so-called "single track model" shown in Fig. 1 (Pilutti et al., 1999; Tseng et al., 1999; Hahn et al., 2004). In Fig. 1, the vehicle sideslip angle β is defined as the angle between the vehicle centerline and the orientation of the vehicle ve-

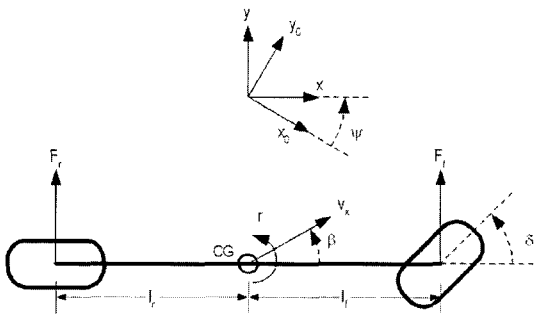

Fig. 1 Single-track model for vehicle lateral dynamics

locity vector, and $r \equiv \dot{\psi}$ is the yaw rate of the vehicle body. The lateral dynamics of a vehicle is controlled by the front wheel steering angle δ_f and the artificial moment input M_{DB} by differential braking.

Defining the body sideslip angle β and the yaw rate $r(\equiv\dot{\psi})$ of the vehicle body as state variables with front wheel steering angle δ_f and control moment M_{DB} as inputs, the vehicle lateral dynamics is described as follows:

$$\dot{\beta}=-r+\frac{C_f}{mv_x}\left(\delta-\beta-\frac{l_f r}{v_x}\right)+\frac{C_r}{mv_x}\left(-\beta+\frac{l_r r}{v_x}\right) \quad (1a)$$

$$\dot{r}=\frac{l_f C_f}{I_z}\left(\delta-\beta-\frac{l_f r}{v_x}\right)-\frac{l_r C_r}{I_z}\left(-\beta+\frac{l_r r}{v_x}\right)+\frac{1}{I_z}M_{DB} \quad (1b)$$

where m is the vehicle mass, v_x is the vehicle longitudinal velocity, I_z is the equivalent yaw moment of inertia, l_f, l_r are the distances from CG (center of gravity) to front and rear wheels, respectively, and C_f and C_r are the cornering stiffness of front and rear tires, respectively.

Using the lateral G sensor signal $a_y(a_y=v_x\dot{\beta}+v_x r)$, the single track model can be re-written by eliminating the body sideslip angle β as follows:

$$\begin{aligned}\dot{r}&=\frac{C_f C_r}{C_f+C_r}\frac{(l_f+l_r)^2}{I_z v_x}r+\frac{m(l_f C_f-l_r C_r)}{(C_f+C_r)I_z}a_y\\&\quad+\frac{C_f C_r}{C_f+C_r}\frac{l_f+l_r}{I_z}\delta+\frac{1}{I_z}M_{DB}\\&=a(v_x,C_f,C_r)\,r+b_1(C_f,C_r)\,a_y+b_2(C_f,C_r)\,\delta\end{aligned} \quad (2)$$

Since the vehicle stability management system is of primary concern, this paper concentrates on the yaw rate dynamics (Eq. (2)) in response to the moment control input M_{DB}. The special feature of this yaw rate dynamic model is that this model contains the measurable lateral G sensor signal a_y rather than immeasurable body sideslip angle β.

3. Robust Yaw Rate Control for Vehicle Stability Management

3.1 Yaw rate control

If driver's steering input, in yaw rate dynamics (Eq. (1)), is assumed to be uncontrollable element, single control input M_{DB} cannot control two state variables β and r of vehicle lateral dynamics simultaneously to each trajectory for all values of time, with an acceptable performance (Skogestad and Postlethwaite, 1996; Nagai et al., 2002). Hence, the control variable, that is either body sideslip β or yaw rate r, needs to be selected. This paper chooses the yaw rate, which can be directly measured by a sensor, to be a control variable and then focuses on the yaw rate control of vehicle, as a main methodology of vehicle stability management. The reference yaw rate used for the feedback control is determined considering the single track model (Eq. (1)) and the physical friction limit (You, 2006). In addition, the stability of the sideslip internal dynamics is investigated as a prerequisite to yaw rate control. Eq. (1) confirms that the sideslip zero dynamics is asymptotically stable.

To maintain the overall lateral stability of a vehicle in real-world application, there also need to be the additional functions of VSM system such as the reduction of body sideslip and the prevention of rollover. Their solutions from the standpoint of yaw rate control can be presented as follows. Similar to the principle of determining the rear steer angle in a 4WS (Four Wheel Steer) system (Whitehead, 1988), the reference yaw rate is assumed to be defined as Eq. (3). Then it changes sideslip dynamics (Eq. (1a)) into its internal dynamics (Eq. (4)), which implies that body sideslip asymptotically converges to zero.

$$r_{ref}=\left(\frac{C_f}{mv_x}\delta_f\right)\Big/\left(1-\frac{C_r l_r-C_f l_f}{mv_x^2}\right) \quad (3)$$

$$\dot{\beta}=-\frac{C_f+C_r}{mv_x}\beta \quad (4)$$

In addition, the risk of rollover can be mitigated by reducing the reference yaw rate toward the understeer way prior to rollover occurrence, which plays the role of diminishing the centrifugal force. According to this method, the braking force is generated in the outer side wheels, which consequently helps the mitigation of rollover since the increase of braking force makes cornering force, i.e. the causal force of rollover, decrease. Conse-

quently, the vehicle body sideslip reduction and the rollover mitigation can be fulfilled, in the light of the yaw rate control, via the proper choice of reference yaw rate.

3.2 Motivation for gain-scheduled robust control and control strategy

The lateral dynamics of a vehicle varies in its characteristics with respect to the change of the following factors: center of gravity, mass, yaw moment of inertia, cornering stiffness, tire-road friction and road bank angle, etc. Moreover, these vehicle parameters incessantly change depending on the number of passengers, vehicle load and road condition, which naturally calls for the real-time estimation of the varying parameters. Although much research has been done using the real-time estimation methods to identify these vehicle parameters, the estimation error is practically unavoidable for several reasons such as their preliminary assumptions, modeling error and measurement noise. Therefore, the controller needs to be robust to maintain its performance and stability against parametric uncertainties and external disturbances.

The lateral dynamic characteristics of a vehicle are also affected by the longitudinal velocity of a vehicle. Therefore, it is not realistic to apply a fixed-gain-type linear controller to real-world application because the single track model, which is used as a baseline model of control design, is LPV (Linear Parameter Varying)-type model with respect to the measurable longitudinal velocity. From these points of view, this paper proposes the H_∞ optimal yaw rate controller coupled with longitudinal-velocity-based gain scheduling so that the aforementioned requirements can be satisfied.

The strategy of the yaw rate control in this paper can be divided into the following two stages. In the yaw rate tracking control problem of this paper, the driver's steer input can be regarded as a known disturbance. Thus, the yaw rate controller, which determines the pseudo control input u, is firstly synthesized in this section without separately considering driver's steer input in the control design as follows:

$$\begin{aligned} \dot{r} &= a(v_x, C_f, C_r)\, r + u \\ u(s) &= K(s)\, e(s) = K(s)\,(r_{ref}(s) - r(s)) \end{aligned} \tag{5}$$

Next, the feed-forward yaw moment resulting from steer input will be considered in the implementation stage of the designed controller. As shown in Eq. (6), the final real compensatory yaw moment M_{DB} assigned to differential braking is the portion excluding the feed-forward terms from the output of designed yaw rate controller, i.e. the pseudo control input.

$$\begin{aligned} M_{DB} = I_z[&K(s)\,(r_{ref} - r) \\ &-\{b_1(C_f, C_r)\, a_y + b_2(C_f, C_r)\, \delta\}] \end{aligned} \tag{6}$$

Therefore, it is noted that the accurate identification of the feed-forward yaw moment generated by steering effect is required for effectively implementing the designed yaw rate controller, which will be presented in Section 4.

3.3 Local H_∞ controller synthesis

In this subsection, local controllers, which maintain the performance and stability only in their own local longitudinal velocity regions, were designed using H_∞ optimization technique.

3.3.1 Formulation

A schematic diagram for robust yaw rate feedback control is shown in Fig. 2, where r_{ref} is the reference yaw rate signal, r is the output yaw rate signal, e is the tracking error, u is the control input signal, u_Δ is the model uncertainty and d is the external yaw moment disturbance signal. Besides, z and r_Δ are frequency-shaped error and plant output signals, respectively. $K(s)$ denotes the feedback controller to be synthesized in this subsection, and $G(s)$ is the plant model. The filters $W_P(s)$ and $W_I(s)$ are frequency shaping functions (or frequency weights) used to mathematically describe the performance and modeling error specifications, respectively. The filter $W_d(s)$ is the yaw-disturbance input-transfer function. Considering the parametric uncertainty concerning $a(v_x, C_f, C_r)$ in Eq. (2) (resulting from the fixed base velocity in the local region and the estimation error of cornering stiffness) and un-

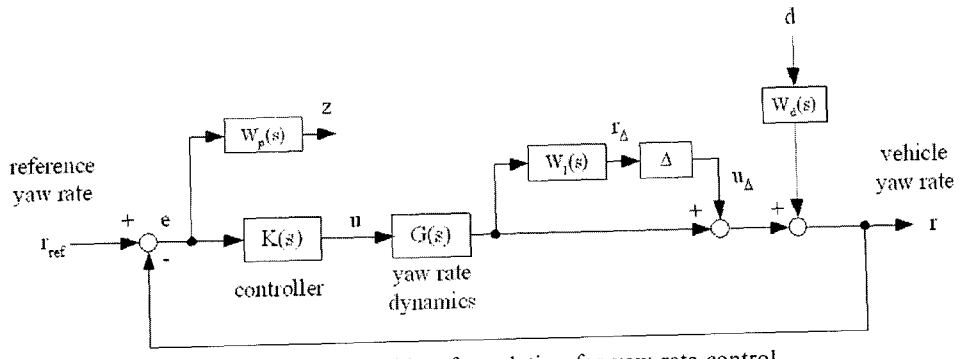

Fig. 2 Control problem formulation for yaw rate control

modeled dynamics, this paper assumes that the plant uncertainty is modeled by the output multiplicative uncertainty (Skogestad and Postlethwaite, 1996; Doyle et al., 1992; Zhou and Doyle, 1998) as shown in Fig. 2.

In Fig. 2, the output yaw rate signal and tracking error are defined as follows:

$$r=\frac{GK(1+W_I\Delta)}{1+GK(1+W_I\Delta)}r_{ref}+\frac{W_d}{1+GK(1+W_I\Delta)}d \tag{7a}$$

$$e=r_{ref}-r=\frac{1}{1+GK(1+W_I\Delta)}r_{ref}-\frac{W_d}{1+GK(1+W_I\Delta)}d \tag{7b}$$

where Δ is an arbitrary stable complex function with $|\Delta(j\omega)|<1$ for all ω.

The sensitivity and complementary sensitivity are also defined as follows:

$$S(s)\equiv\frac{e(s)}{r_{ref}(s)}=\frac{1}{1+G(s)K(s)} \tag{8a}$$

$$T(s)\equiv\frac{r(s)}{r_{ref}(s)}=\frac{G(s)K(s)}{1+G(s)K(s)} \tag{8b}$$

$$S_p(f)\equiv\frac{e(s)}{r_{ref}(s)}=[1+G(s)K(s)(1+W_I(s)\Delta(s))]^{-1} \tag{8c}$$

$$T_p(s)\equiv\frac{r(s)}{r_{ref}}=G(s)K(s)(1+W_I(s)\Delta(s))[1+G(s)K(s)(1+W_I(s)\Delta(s))]^{-1} \tag{8d}$$

where the subscript 'p' implies that the transfer functions are not nominal but perturbed.

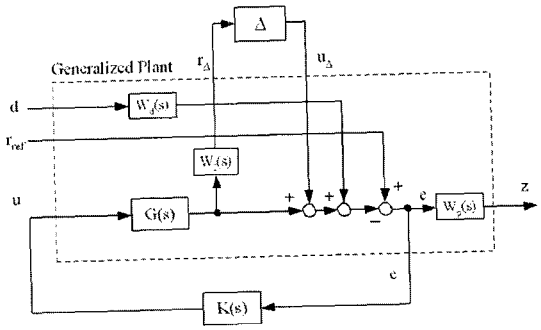

Fig. 3 Generalized plant

The corresponding generalized plant (Balas et al., 2001; Gahinet et al., 1995) **P**, which has inputs $[u_\Delta\ r_{ref}\ d\ u]^T$ and outputs $[r_\Delta\ z\ e]^T$, can be derived by inspecting Fig. 3:

$$\begin{bmatrix}r_\Delta\\ z\\ e\end{bmatrix}=P\begin{bmatrix}u_\Delta\\ r_{ref}\\ d\\ u\end{bmatrix}=\begin{bmatrix}0 & 0 & 0 & W_IG\\ -W_p & W_p & -W_pW_d & -W_pG\\ -1 & 1 & -W_d & -G\end{bmatrix}\begin{bmatrix}u_\Delta\\ r_{ref}\\ d\\ u\end{bmatrix} \tag{9}$$

where $u(s)=K(s)e(s)$.

For $N\Delta$-structure (Skogestad and Postlethwaite, 1996), the nominal system N, which is the closed-loop transfer function from inputs $[u_\Delta\ r_{ref}\ d]^T$ to outputs $[r_\Delta\ z]^T$, can be derived using lower linear fractional transformation (LFT) (Skogestad and Postlethwaite, 1996; Zhou and Doyle, 1998):

$$N=F_l(P,K)\triangleq P_{11}+P_{12}K(I-P_{22}K)^{-1}P_{21}=\left[\begin{array}{c|cc}N_{11} & N_{12}\\ \hline N_{21} & N_{22}\end{array}\right]=\left[\begin{array}{c|cc}-W_IT & W_IT & -W_IW_dT\\ \hline -W_pS & W_pS & -W_pW\end{array}\right] \tag{10}$$

where $\mathbf{P}=\left[\begin{array}{c|cc}P_{11} & P_{12}\\ \hline P_{21} & P_{22}\end{array}\right]=\left[\begin{array}{ccc|c}0 & 0 & 0 & W_IG\\ -W_p & W_p & -W_pW_d & -W_pG\\ \hline -1 & 1 & W_d & -G\end{array}\right]$.

Similarly, the uncertain closed-loop transfer function from $[r_{ref}\ d]^T$ to z, $z=F[r_{ref}\ d]^T$, is related to N and Δ by an upper LFT,

$$\begin{aligned} F&=F_u(N,\Delta)\triangleq N_{22}+N_{21}\Delta(I-N_{11}\Delta)^{-1}N_{12}\\ &=[W_pS_p\ -W_pS_pW_d]\\ &=\left[\frac{W_p}{1+GK(1+W_I\Delta)}-\frac{W_pW_d}{1+GK(1+W_I\Delta)}\right] \end{aligned} \tag{11}$$

For achieving robust performance in the problem in Fig. 2, the following condition should be satisfied:

$$\|F\|_\infty<1,\ \forall\Delta,\ \forall\omega \tag{12}$$

where $\|F\|_\infty$ can be defined as follows (because $\|F\|_\infty$ is a vector, not a matrix):

$$\begin{aligned} \|F\|_\infty&=\max_\omega\sqrt{|W_pS_p|^2+|W_pW_dS_p|^2}\\ &=\max_\omega\sqrt{1+|W_d|^2}\,|W_pS_p| \end{aligned} \tag{13}$$

From the definition in Eqs. (12) and (13), the robust performance criterion can be rewritten as follows:

$$\max_\Delta\sqrt{1+|W_d|^2}\,|W_pS_p|<1,\ \forall\omega \tag{14}$$

Since the worst-case is obtained at each frequency by selecting $|\Delta(j\omega)|=1$ such that the denominator of the perturbed sensitivity function S_p is minimized, the final robust performance condition becomes:

$$|W_IT|+\sqrt{1+|W_d|^2}\,|W_pS|<1,\ \forall\omega \tag{15}$$

by the following formulations:

$$\begin{aligned} \max_\Delta\sqrt{1+|W_d|^2}\,|W_pS_p|&=\sqrt{1+|W_d|^2}\,\frac{|W_p|}{|1-L|-|W_IL|}\\ &=\sqrt{1+|W_d|^2}\,\frac{|W_pS|}{1-|W_IT|} \end{aligned}$$

The inequality in Eq. (15) can be practically approximated by the following mixed sensitivity H_∞ problem:

$$\max_K\left\|\begin{matrix} W_pS\\ W_dW_pS\\ W_IT\end{matrix}\right\|_\infty \tag{16}$$

Finally, the robust controller K(s), which tightly satisfies the performance and robustness condition (Eq. (15)), is mathematically synthesized by Eq. (16).

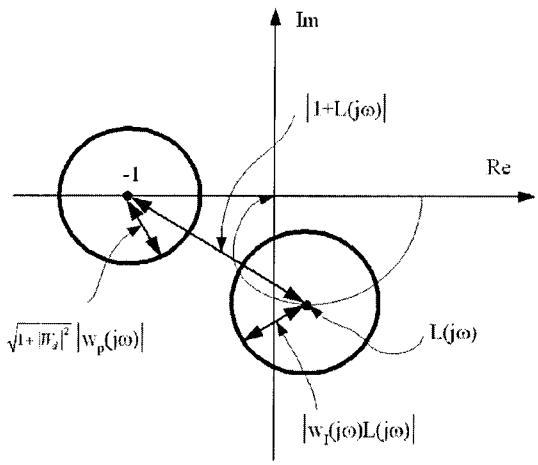

Fig. 4 Nyquist plot for robust performance condition

Besides, if the nominal stability requirement, i.e. N is stable, is satisfied, we have that

$$\begin{aligned} &\|F\|_\infty=\|F_u(N,\Delta)\|_\infty<1,\ \forall\Delta,\ \forall\omega\\ &\quad\Longleftrightarrow\mu_{\hat\Delta}(N(j\omega))<1,\ \forall\omega\\ &\hat\Delta=\begin{bmatrix}\Delta & 0 & 0\\ 0 & \Delta_{p1} & \Delta_{p2}\end{bmatrix}^T,\ \|\hat\Delta\|_\infty<1 \end{aligned} \tag{17}$$

where μ is defined with respect to the structured uncertainty $\hat\Delta$ and $[\Delta_{p1}\ \Delta_{p2}]^T$ is a full complex perturbation with the same dimensions as F^T.

Therefore, the structured singular value $\mu(N)$ can be derived as follows:

$$\therefore\mu(N)=|W_IT|+\sqrt{1+|W_d|^2}\,|W_pS| \tag{18}$$

This robust performance condition can be also illustrated on the Nyquist plot as shown in Fig. 4.

3.3.2 Control design

Specifying the performance and robustness requirements is a crucial stage in the H_∞ controller design. In particular, it is essential to accurately define the amount of uncertainty inherent in the plant to be controlled, since the performance specification is closely related to the uncertainty. This subsection proposes the velocity-based gain scheduling approach, which designs several local controllers for each velocity interval, as a methodology to compensate the variation of yaw rate

dynamics by longitudinal velocity. The amount of plant parametric uncertainty which the individual local controller should cover is more or less tunable element since it depends on the number of the designed local controllers.

Based on the number of designed local controllers and the parametric uncertainty, this paper assumes that the amount of uncertainty increases from 20% at low frequency range, reaching 230% at high frequency range, which can be succinctly described by the following frequency shaping function $W_I(s)$:

$$W_I(s) \equiv \frac{s+\omega_2 A_2}{\frac{s}{M_2}+\omega_2} = \frac{s+90\times 0.2}{\frac{s}{2.3}+90} \qquad (19)$$

It is noted that the amount of uncertainty of 230% at high frequency region is arbitrarily chosen but can be adjusted without violating the robust performance criterion stated in Eq. (15).

Before defining the performance requirements, the open-loop transfer function $W_d(s)$ from yaw moment disturbance d to output yaw rate r is assumed to be the nominal yaw rate dynamics.

Given the amount of uncertainty, the next step is to select the shaping function for the performance specification. In this paper, the frequency shaping function for the performance specification is selected for the closed-loop system to achieve the following requirements: 1) to keep the steady-state yaw rate tracking error as small as possible, 2) to reject the yaw moment disturbances on the yaw motion of the vehicle, 3) to imitate the speed of yaw rate response by driver's steer input in a passive system in low-frequency range and 4) to limit compensatory braking force up to friction margin.

To minimize steady-state tracking error, $W_P(s)$ assumes 10^2 at DC (0 Hz), which is equivalent to 1% steady-state error. Other parameters of $W_P(s)$ in Eq. (20) are chosen so that the closed loop system meets the above-mentioned requirements as well as guarantees the robust performance criterion (Eq. (15)):

$$W_P(s) = \frac{\frac{s}{M_1}+\omega_1}{s+\omega_2 A_1} = \frac{\frac{s}{3}+7}{s+7\times 10^{-2}} \qquad (20)$$

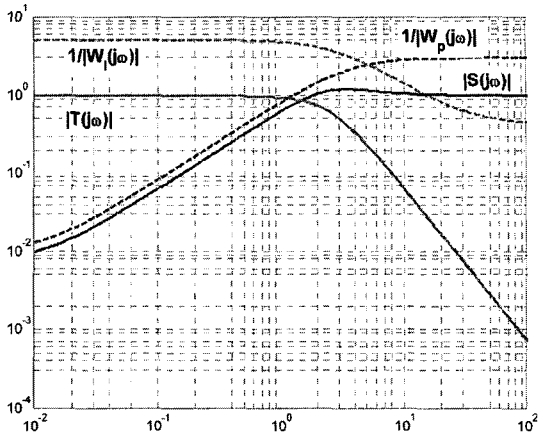

Fig. 5 Shaping functions for controller design

It is noted that simple first order filters are used to define the frequency shaping functions to keep the order of controller as small as possible, since the order of the H_∞ controller is equal to that of the generalized plant (Zhou and Doyle, 1998).

Equipped with two shaping functions and the generalized plant (Eq. (9)), the designed local H_∞ controller with respect to 100 km/h is as follows:

$$K(s) = \frac{289.9s^3+61682s^2+612976s+1559586}{s^4+256.1s^3+7339s^2+31470s+2331} \qquad (21)$$

Figure 5 shows the sensitivity and complementary sensitivity functions obtained using the designed local H_∞ controller, along with the frequency shaping functions. The gain and phase margins of the resulting loop gain are inf dB and 71.5°, respectively. The resulting closed-loop transfer function achieves its bandwidth of approximately 2.15 Hz. The structured singular value $\mu(N)$ is 0.97, which is strictly less than unity (which means the robust performance objective is satisfied).

3.4 Global control design

In general, the large model uncertainty allowed for control design necessarily results in the performance degradation, due to trade-offs between the performance and robustness. Accordingly, the key point for maximizing the performance of control system is to minimize the model uncertainty in the viewpoint of robust performance.

The fact that vehicle longitudinal velocity can be measured makes it possible to apply the velocity-based gain scheduling approach and it is beneficial to improve the performance of yaw rate controller. In other words, the longitudinal velocity v_x is regarded, in the baseline yaw rate dynamic model (Eq. (2)), as a known time-varying parameter rather than an uncertain one as it can be easily measured.

The longitudinal velocity scope considered in this paper is between 25 km/h to 180 km/h and the base velocities for gain scheduling are appropriately determined considering the model uncertainty defined in the previous subsection. For each base velocity, the local H_∞ optimal controller is synthesized according to the proposed procedure in the previous subsection. Finally, the global controller with velocity-based gain scheduling, which can cover the whole velocity region through switching the local controllers based on the vehicle longitudinal velocity and vehicle parameters, is implemented to yaw rate control system for stabilizing vehicle lateral dynamics as shown in Fig. 6.

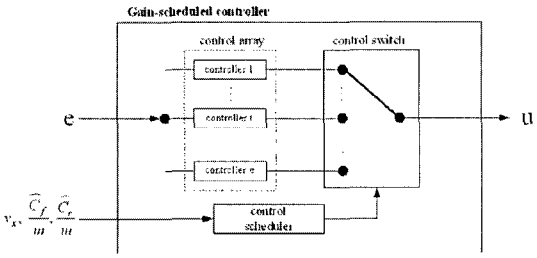

Fig. 6 Schematics of global gain-scheduled controller

4. Implementation of Yaw Rate Controller

This section deals with the implementation of the designed yaw rate controller. First of all, the feed-forward yaw moment generated by driver's steer input is estimated through disturbance observer and then, the compensatory yaw moment M_{DB} assigned to differential braking is determined by excluding the feed-forward terms from the output of designed yaw rate controller, i.e. the pseudo control input. The next process is concerned with deciding how braking forces should be distributed to the individual wheels in order to generate the target compensatory yaw moment. The schematic diagram of the implemented yaw rate control system is shown in Fig. 7 and these processes are further explained in more detail in the subsequent sections.

4.1 Disturbance observer design for estimating the feed-forward yaw moment

To effectively implement the designed yaw rate controller, the reliable identification of the feed-forward terms $b_1a_y+b_2\delta$ at first, is a prerequi-

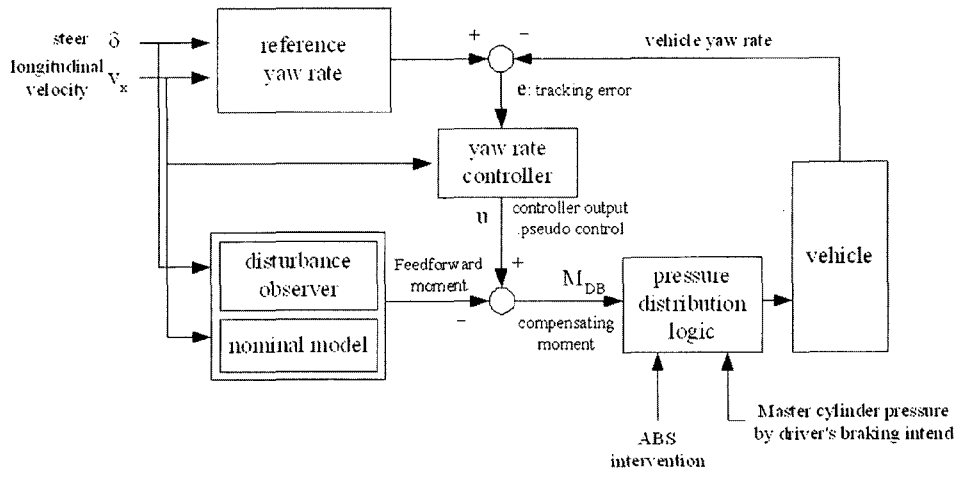

Fig. 7 Schematic diagram of yaw rate control system

site since the derivation process of target control moment $M_{DB,ref}$ requires it as shown in Eq. (6).

$$M_{DB,ref}=I_z[K(s)(r_{ref}-r) -\{b_1(C_f,C_r)a_y+b_2(C_f,C_r)\delta\}] \quad (6)$$

It should be noted that the estimation of these feed-forward terms is a challenging task in that the coefficients a, b_1, b_2 are unknown time-varying parameters and the generated compensating yaw moment M_{DB}/I_z is not also available in real-world application. For the activation of the vehicle stability management system, the vehicle yaw rate dynamics model is given by Eq. (22).

$$\begin{aligned}\dot{r}&=-\frac{C_fC_r}{C_f+C_r}\frac{(l_f+l_r)^2}{I_zv_x}r+\frac{m(l_fC_f-l_rC_r)}{(C_f+C_r)I_z}a_y \\ &+\frac{C_fC_r}{C_f+C_r}\frac{l_f+l_r}{I_z}\delta+\left(\frac{M_{DB}}{I_z}\right) \\ &=ar+b_1a_y+b_2\delta+\left(\frac{M_{DB}}{I_z}\right)\end{aligned} \quad (22)$$

Considering parametric uncertainties, yaw rate dynamic model can be divided into two parts, i.e., known nominal terms and perturbed terms, as follows:

$$\begin{aligned}\dot{r}&=a_nr+b_{1,n}a_y+b_{2,n}\delta+\left(\frac{M_{DB}}{I_z}\right)_n \\ &+\left\{(\Delta a)r+(\Delta b_1)a_y+(\Delta b_2)\delta+\Delta\left(\frac{M_{DB}}{I_z}\right)\right\}\end{aligned} \quad (23)$$

where $M_{DB}|_n(=T_{tread}\cdot K_B\cdot P_{DB}/2r_{tire})$ is the nominal value of the compensatory yaw moment generated by differential braking, T_{tread} is the vehicle tread, K_B is the brake gain from braking pressure to braking torque defined by friction coefficient, friction area and effective friction radius, P_{DB} is the differential braking pressure and r_{tire} is the tire radius.

The on-line parameter estimation method based on adaptive approach can be applied to identify the parametric uncertainties but it is difficult to implement the adaptive approach into yaw rate dynamics because the four uncertain parameters themselves are too many to assure the successful parameter adaptation, in other words, the excitation signal such is not sufficiently rich enough to identify all the parameters in yaw rate dynamic model. Moreover, these parameters do not need to be respectively estimated in the viewpoint of yaw rate control since their uncertainties work in a lump on the yaw rate dynamics.

Therefore, this paper simplifies the estimation problem by unifying the perturbed terms in Eq. (23) into one disturbance w as shown in Eq. (24) and proposes the disturbance observer to identify the lumped disturbance w.

$$w=\Delta\left(\frac{M_{DB}}{I_z}\right)+\{(\Delta a)r+(\Delta b_1)a_y+(\Delta b_2)\delta\} \quad (24)$$

Assuming disturbance dynamics is sufficiently slow, disturbance w is augmented to the state r to yield a new state variable $\mathbf{x}$ defined as follows:

$$\mathbf{x}=[r\ w]^T \quad (25)$$

With the state vector given by Eq. (25), vehicle yaw rate dynamics (Eq. (22)) takes the state space representation shown below:

$$\begin{aligned}\frac{d}{dt}\mathbf{x}&=\begin{bmatrix}a_n & 1\\ 0 & 0\end{bmatrix}\mathbf{x}+\begin{bmatrix}b_{1,n} & b_{2,n} & \frac{K_B}{I_z}\\ 0 & 0 & 0\end{bmatrix}\begin{bmatrix}a_y\\ \delta\\ P_{DB}\end{bmatrix} \\ &=\mathbf{A}_d\mathbf{x}+\mathbf{B}_d\mathbf{u}\end{aligned} \quad (26a)$$

$$\mathbf{y}=[1\ 0]\mathbf{x}=\mathbf{C}_d\mathbf{x} \quad (26b)$$

Then, the corresponding disturbance observer to estimate $\mathbf{x}$ is given by the Luenberger-type observer (Eq. (27)), where $\mathbf{L}_d$ is the feedback gain matrix (Hahn et al., 2004):

$$\frac{d}{dt}\hat{\mathbf{x}}=\mathbf{A}_d\hat{\mathbf{x}}\mathbf{B}_d\mathbf{u}+\mathbf{L}_d(\mathbf{y}-\mathbf{C}_d\hat{\mathbf{x}}) \quad (27)$$

By a proper choice of the feedback gain matrix $\mathbf{L}_d$, the simultaneous exponential convergence of both state variable and disturbance to zero can be guaranteed. Using the estimated lumped disturbance by the above-mentioned disturbance observer, the resulting compensatory yaw moment that should be assigned to differential braking can be finally represented as follows:

$$M_{DB,ref}=I_{z,n}[K(s)(r_{ref}-r)-(b_{1,n}a_y+b_{2,n}\delta)-\hat{w}] \quad (28)$$

4.2 Brake force distribution

This subsection deals with the determination of efficiency order in braking wheels and braking release wheels, and the distribution priority of braking force. As presented in Section 2.2, tire

force exists within the friction circle on the plane and its longitudinal and lateral components are coupled with each other. Specifically, lateral force decreases with the increase of longitudinal force, and its maximum value is defined by the longitudinal force (Koibuchi et al, 1996; Peng et al., 2000). In this respect, it can be noted that there exist one efficient braking wheel even between the same side wheels, which yield the same directional yaw moment, since braking pressure for generating the designed artificial yaw moment affects the lateral tire force as well as the longitudinal tire force.

In case of an understeering situation, it is desirable to generate the compensatory braking force at the rear-inner wheel, because the braking force at the front-inner wheel makes a reduction in the lateral force of the corresponding wheel and this consequently cancels the compensatory yaw moment. In the viewpoint of friction margin, it is effective in the understeering motion to brake the rear-inner wheel which has more friction margin, since the understeering motion mainly results from the excessive sideslip of front wheels, i.e. the saturation of lateral force of front wheels. On the other hand, the oversteering motion is caused by the large sideslip of rear wheels beyond the linear friction region and the braking force at the rear-outer wheel makes a reduction in the lateral force of the corresponding wheel, which also cancels the compensatory yaw moment. Thereby, the braking force in the front-outer wheel is required to overcome the oversteering situation. In addition, the optimal braking wheels are determined not by the sign of steer input, but according to the direction of lateral force in each wheel. This point implies that all two wheels in the same side may be the optimal wheels when the direction of front and rear lateral forces is opposite.

So far, the cases where drivers do not operate their brakes are considered only. But, most drivers operate the brake pedal in the critical driving situation, and thus the releasing braking pressure, apart from generating braking pressure, can be also applicable to the yaw moment intervention. Under braking situations by drivers' maneuver, there is the optimal braking release wheel according to the same principle as mentioned above. Tables 1 and 2 arrange the optimal braking wheel and releasing wheel for the respective cornering situation.

As discussed above, the braking intervention to the optimal wheel for the compensatory yaw moment yields additional moment due to the reduction of lateral force as well as the moment $M = \Delta F_x \cdot T_{tread}/2$ by the braking force variation.

Table 1 Optimal braking wheel on driving conditions

Optimal braking wheel	Driving Conditions	
	Desired yaw moment	Lateral force
Front Left Wheel (FL)	counterclockwise	to right
Front Right Wheel (FR)	clockwise	to left
Rear Left Wheel (RL)	counterclockwise	to left
Rear Right Wheel (RR)	clockwise	to right

Table 2 Optimal releasing wheel on driving conditions

Optimal braking wheel	Driving Conditions	
	Desired yaw moment	Lateral force
Front Left Wheel (FL)	clockwise	to right
Front Right Wheel (FR)	counterclockwise	to left
Rear Left Wheel (RL)	clockwise	to left
Rear Right Wheel (RR)	counterclockwise	to right

Hence, it is only natural to investigate the problem relating to how this plus-something effect on the yaw rate dynamic model should be considered. A simple method is defining the target braking force variation smaller than the originally-designed force $M_{DB,ref} \cdot 2/T_{tread}$, in expectation of the extra effect. But this approach is not suitable for the model-based control methodology. The indirect moment change by the lateral force variation should be dealt with in the dynamic model because the lateral force has been already represented by the vehicle parameters, such as cornering stiffness, in the yaw rate dynamic model. In this paper, therefore, the variation of lateral force by longitudinal braking force change is compensated by the estimated lumped-disturbance in Eq. (27). The resulting target braking force variation in the optimal braking wheel can be expressed as follows:

$$\begin{aligned}\Delta F_{x,ref} &= \frac{2}{T_{tread}} M_{DB,ref} \\ &= 2\frac{I_{z,n}}{T_{tread}}[K(s)(r_{ref}-r)-(b_{1,n}a_y+b_{2,n}\delta)-\hat{w}]\end{aligned} \tag{29}$$

Occasionally, there may be a case where the target braking force exceeds the friction limit, especially on the low friction road. In this case, the short amount of the compensatory moment can be supplemented by braking force in other wheels chosen by an intervention priority. If the braking force at the optimal braking wheel is insufficient due to friction limit in case of no braking input by driver, the additional braking force at the same side wheel compensate the shortage of control moment. Furthermore, when the driver applies braking maneuver, the priority of braking intervention can be defined as follows. Firstly, it should be determined whether the additional braking force and subtractive braking force in the optimal braking/releasing wheels for generating the target yaw moment remain or not. In this point, the important constraints are that the sum of overall braking force should correspond to driver's braking command, if possible, in order to minimize the effect of yaw moment intervention to the vehicle longitudinal dynamics. If there is still a shortage of control moment in spite of using the optimal braking/releasing wheels, the remaining target moment is generated through the extra braking in the same side wheel and the extra braking release in the next wheel. The aforementioned priority of braking force distribution is shown in Table 3.

The determined target braking force at the individual wheel is realized by the pressure control in the brake chamber. The pressure control method used in this paper is detailed in (You et al., 2006). By assuming that the dynamics from braking pressure to the braking torque, i.e. wheel dynamics, is fast enough to neglect itself, compared with vehicle yaw dynamics, the target braking pressure at the individual wheel can be given as shown in Eq. (30).

$$P_{ref,i} = r_{tire,i}\frac{F_{ref,i}}{K_{B,i}};\ i=FL,FR,RL,RR \tag{30}$$

5. Hardware-In-the-Loop-Simulation

In this section, several HILS (Hardware-In-the-Loop-Simulation) results are presented to verify the performance of the proposed vehicle stability management system based on the yaw rate control. For the reliability of the vehicle model in HILS, CarSim software, which is one of the most-used commercial softwares, was used for performing the vehicle dynamics simulation portion of HILS.

Table 3 Brake intervention priority

Priority	Brake intervention sequence
1	Optimal braking/releasing wheel
2	Alternative braking/releasing wheel
Constraint: no intervention in vehicle longitudinal dynamics (the sum of the overall braking force should correspond to driver's braking command)	

5.1 Control intervention criterion and driver model

This subsection defines the control intervention criterion used in this paper. It should be noted that even the control characteristics of the same VSM logic vary from one another according to the intervention timing (Chung and Yi, 2005). When only vehicle stability is considered, the full-time control, which is activated even by the slight vehicle sideslip, is desirable. However, a driver may feel awkward from the frequent and nuisance activation of VSM system since the current vehicle stability management system is recognized by the driver as a driver assistance system. In this respect, it is required that VSM system is activated only when deemed necessary.

In this study, the intervention condition is defined by the following two criterions.

(1) The VSM system is activated, from the standpoint of yaw rate, when the error between the actual yaw rate and theoretical yaw rate exceeds a specific value. An apparent discrepancy between these two yaw rates means that the nonlinear friction is caused by the lateral force saturation either in the front wheels or in the rear wheels. Thus, the proper yaw moment intervention is required for mitigating the excessive tire sideslip in the front and/or rear wheels.

(2) Since the inordinate body sideslip implies the excessive lateral slip of front or rear wheels, the body sideslip angle needs to fall within certain limits via the adequate intervention of VSM system. When the intervention commences by this criterion, the target yaw rate shifts from the conventional theoretical yaw rate to Eq. (3) as presented in Section 3.1.

The understeering situation requires the faster intervention in that the main intervention wheels of the understeered vehicle, i.e. inner-side wheels, is apt to have insufficient margin of additive braking force due to the lateral load transfer. Furthermore, the offset is applied to the activation/deactivation condition for preventing the chattering of interventions.

According to our HILS study, the characteristics of the overall vehicle lateral motion turned out to significantly depend on the driver model as well as the control intervention criterion mentioned above. This paper exploits the UMTRI (University of Michigan Transportation Research Institute) preview driver model (MacAdam, 1980), which was proposed in 1980 by MacAdam, for the path tracking cases. This driver model is known as an optimal steer model to minimize the difference between the target path and the predicted vehicle path.

5.2 HILS setup

Figure 8 shows the schematic diagram of the HILS set-up, which consists of a hydraulic unit, a hydraulic power pack, pressure transducers, a PC-based real-time interface system for data acquisition and feedback control, and CarSim RT as a vehicle simulator.

The hydraulic module in a luxury sedan with a 4.5 liter, V8 engine is used as a hydraulic unit. A dSPACE equipment is employed to acquire

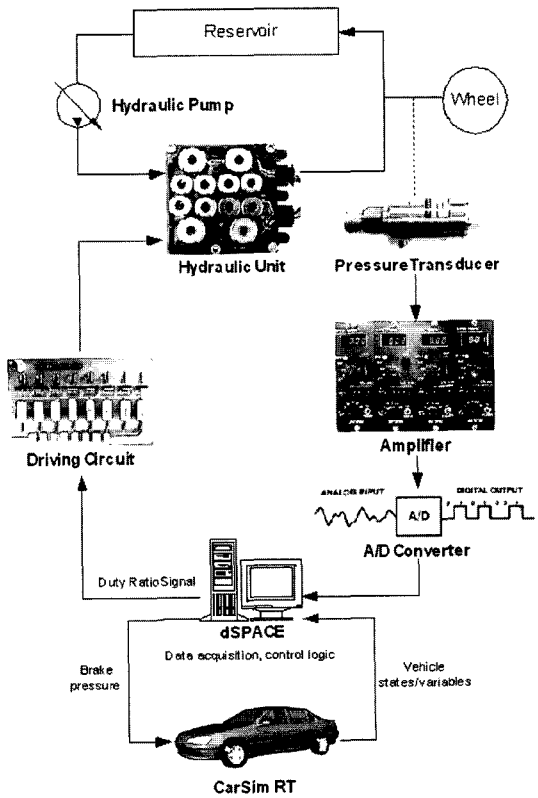

Fig. 8 Schematic diagram of HILS setup

data and implement the control law. The sampling rate in this study is 100 Hz, which is enough to implement the proposed algorithm in real-world applications. The oil inflow from the hydraulic power pack is controlled by the solenoid valves in the hydraulic module shown in Fig. 8 to build the wheel brake pressure. The solenoid valves are actuated by 12 V level PWM signals whereas the PWM output signals from the controller are confined to 5 V level, which naturally calls for a driver circuit between the dSPACE equipment and the hydraulic unit in order to adjust the voltage and current levels to these solenoid valves. The pressure transducer monitors the pressure in the brake chamber, which is, after passing through the strain amplifier, fed to the controller as a digital signal through the analog-to-digital converter. An H_∞ controller (which is not detailed in this paper) is designed for the closed-loop pressure control.

5.3 HILS results

Table 4 summarizes the driving condition for several tests presented in this subsection. The results of HILS can be classified into the following two types according to whether the driver model is included or not.

(1) To verify the control performance from the viewpoint of the overall vehicle-driver system, the target path tracking tests, which are based on the driver model presented in Section 5.1, were carried out (Cases 1-3). The pertinence of moment intervention in each case can be assessed mainly through its path error.

(2) To estimate the relevancy of yaw rate control in the driving scenario with the typical driver's steer input, fishhook maneuver, the open-loop steer test was performed (Case 4). The yaw rate tracking error represents the performance of yaw rate control in this case.

Figures 9 and 10 show the path trajectories and controlled brake pressure trajectories in double/single lane change test without driver's brake maneuver (Cases 1 and 2). It is noted that the vehicle drifts away from the target path due to

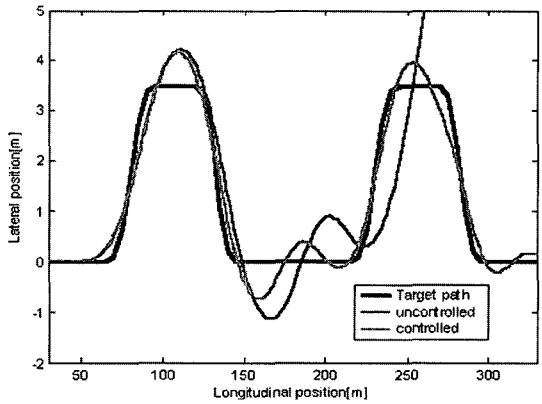

(a) Path trajectories

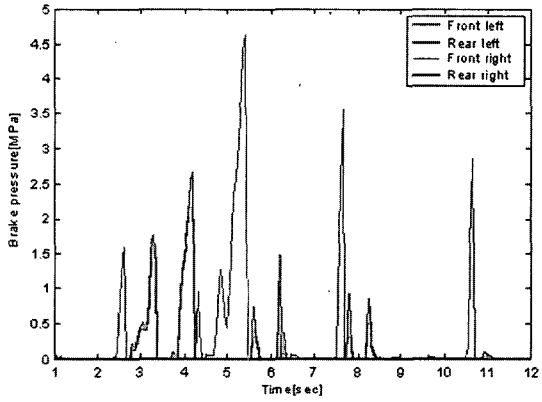

(b) Brake pressure trajectory

Fig. 9 HILS result of double lane change test (Case 1)

Table 4 Driving scenarios

Case	scenario	Longitudinal speed	Road friction
Case 1	Double lane change	120 km/h	0.9
Case 2	Lane change on split mu road	100 km/h	0.2L/0.9R
Case 3	Lane change with full braking (4-7 sec)	50 km/h	0.15
Case 4	Fish-hook	100 km/h	0.9

the rapid and excessive sideslip in front wheel or rear wheel, in case of no activation of VSM system. Through the proper moment intervention by differential braking, consequently, the yaw rate controller maintains the tire grips and enables the vehicle to track the target path well. Especially, Fig. 10 shows that the designed VSM system performs well even in the split-mu road (Case 2).

Figure 11 represents the path trajectories and controlled brake pressure trajectories in lane change test with driver's brake maneuver (Case 3). By adding or subtracting the proper braking pressure in compliance with the priority proposed in Table 3, VSM system helps the vehicle stop without showing any excessive drifts away from the target path, in spite of driver's brake maneuver on the low-mu road surface. The results show that conventional ABS (without consideration of vehicle lateral motion) can restore the stability of the only individual wheel from wheel locking, but can not maintain vehicle lateral stability effectively. It should be noted that this case was carried out through a pure simulation due to the limitation of experimental setup.

Furthermore, the HILS result of the open-loop steer test (Case 4) is shown in Fig. 12. From this result, it is seen that the synthesized yaw rate controller, compared with the case where there is no yaw rate control, enables the controlled vehicle to track the target yaw rate in a satisfactory manner and also with restrained body sideslip. Consequently, the controlled vehicle is safely driven according to driver's steer will since it can maintain the tire grip through the proper yaw moment intervention by differential braking.

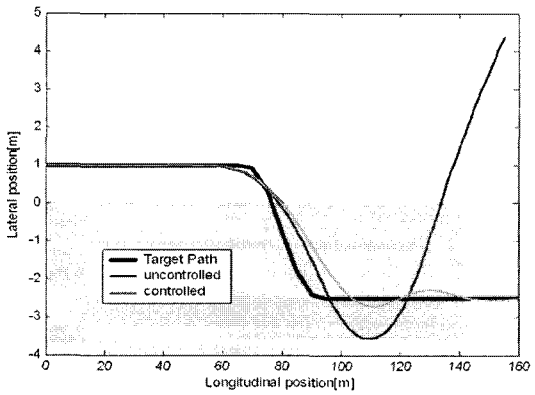

(a) Path trajectories

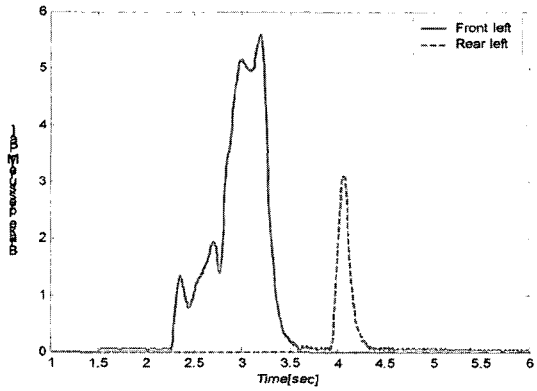

(b) Brake pressure trajectory

Fig. 10 HILS result of lane change test on the split-mu road (Case 2)

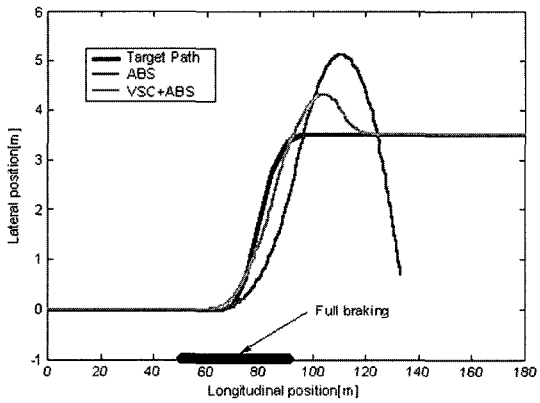

(a) Path trajectories

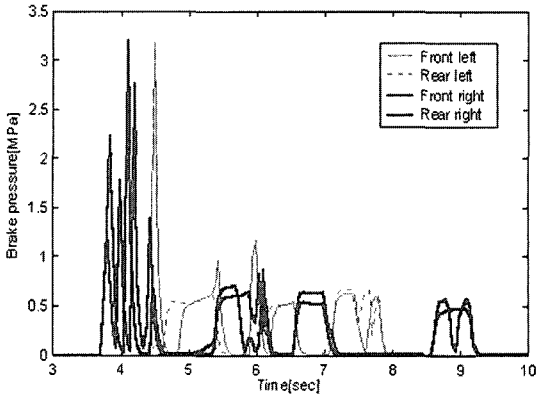

(b) Brake pressure trajectory

Fig. 11 Simulation result of double lane change test with braking (Case 3)

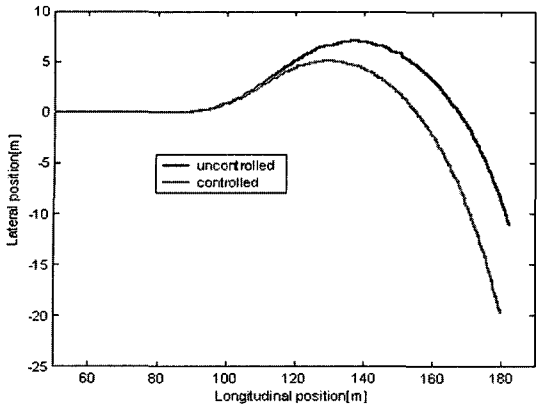

(a) Path trajectories

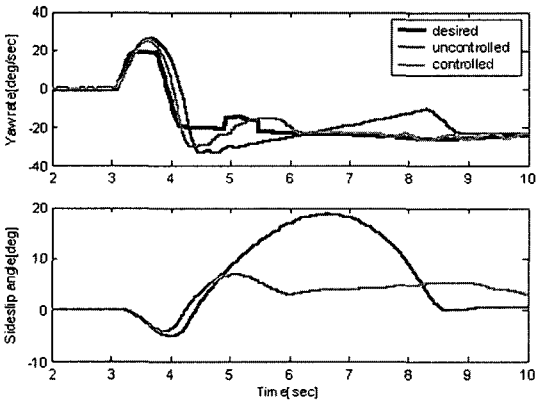

(b) The responses of yaw rate and body sideslip

Fig. 12 HILS result of fish-hook test (Case 4)

6. Conclusions

This paper presents a newly designed yaw rate controller based on gain-scheduled H_∞ optimal control, which not only maintains the rotational vehicle stability, but also has the functions of the reduction of sideslip and the prevention of vehicle rollover. The uncertain factors such as vehicle mass and cornering stiffness in the vehicle yaw rate dynamics naturally call for the robustness of the feedback controller and thereby, H_∞ optimization technique is applied to synthesize a controller with guaranteed robust stability and performance against the model uncertainty. In the implementation stage, the feed-forward yaw moment by driver's steer input is estimated by the disturbance observer in order to determine the accurate compensatory moment. The braking force at the individual wheels for generating artificial yaw moment is distributed according to the braking/braking release efficiency order of the individual wheel and intervention priority, which are based on the interaction between lateral tire force and longitudinal tire force. Finally, HILS results for the various driving conditions reveal that the proposed gain-scheduled robust controller can satisfactorily improve the lateral stability of an automobile.

Acknowledgements

This research was supported by a grant from the BK-21 Program for Mechanical and Aerospace Engineering Research at Seoul National University.

References

Balas, G. J., Doyle, J. C., Glover, K., Packard, A. and Smith, R., 2001, *μ-Analysis and Synthesis Toolbox User's Guide*, MathWorks.

Chung, T. and Yi, K, 2005, "Side Slip Angle Based Control Threshold of Vehicles Stability Control System," *Journal of Mechanical Science and Technology*, Vol. 19, No. 4, pp. 985~992.

Doyle, J. C., Francis, B. A. and Tannenbaum, A. R., 1992, *Feedback Control Theory*, Macmillan Publishing Company.

Gahinet, P., Nemirovski, A., Laub, A. J. and Chilali, M., 1995, *LMI Control Toolbox User's Guide*, MathWorks.

Hahn, J. O., Rajamani, R., You, S. H. and Lee, K. I., 2004, "Real-Time Identification of Road Bank Angle Using Differential GPS," *IEEE Trans. Control Systems Technology*, Vol. 12, pp. 589~599.

Koibuchi K., Yamamoto M., Fukada Y. and Inagaki S., "Vehicle Stability Control in Limit Cornering by Active Brake," SAE960487.

Langwieder, K., Gwehenverger, J., Hummel, T. and Bende, J., 2003, "Benefit Potential of ESP in Real Accident Situations Involving Cars and Trucks," SAE 2003-06-0033.

MacAdam, C. C., 1980, "An Optimal Preview Control for Linear Systems," *Journal of Dynamic Systems, Measurement and Control, ASME*, Vol.

102, No. 3, pp. 188~190.

Nagai, M., Shino, M. and Gao, F., 2002, "Study on Integrated Control of Active Front Steer Angle and Direct Yaw Moment," *JSAE Review*, Vol. 23, pp. 309~315.

Nishimaki, T., Yuhara, N., Shibahata, Y. and Kuriki, N., 1999, "Two-Degree-of-Freedom Hydraulic Pressure Controller Design for Direct Yaw Moment Control System," *JSAE Review*, Vol. 20, pp. 517~522.

Pilutti, T., Ulsoy, G. and Hrovat, D., 1998, "Vehicle Steering Intervention through Differential Braking," *ASME J. Dynamic Systems, Measurement and Control*, Vol. 120, pp. 314~321.

Rieth, P. E. and Schwarz, R., 2004, "ESC II — ESC with active steering intervention," SAE 2004-01-0260.

Skogestad, S. and Postlethwaite, I., 1996, *Multivariable Feedback Control*, John Wiley & Sons.

Tseng, H. E., Ashrafi, B., Madau, D., Brown, T. A. and Recker, D., 1999, "The Development of Vehicle Stability Control at Ford," *IEEE/ASME Trans. Mechatronics*, Vol. 4, pp. 223~234.

Van Zanten, A. T., Erhardt, R., Landesfeind, K. and Pfaff, G., 1998, "VDC Systems Development and Perspective," SAE 980235.

Whitehead, J. C., 1988, "Four Wheel Steering : Maneuverability and High Speed Stabilization," SAE Paper 880642.

Yasui, Y., Tozu, K., Hattori, N. and Sugisawa, M., 1996, "Improvement of Vehicle Directional Stability for Transient Steering Maneuvers Using Active Brake Control," SAE 960485.

You, S. -H., 2006, "Modeling, Estimation and Control of a Vehicle Stability Management System," Ph.D. Thesis, School of Mechanical and Aerospace Engineering, Seoul National University.

You, S. -H., Hahn, J. -O., Cho, Y. M. and Lee, K. I., 2006, "Modeling and Control of a Hydraulic Unit for Direct Yaw Moment Control in an Automobile," *Control Engineering Practice*, accepted for publication.

Zhou, K. and Doyle, J. C., 1998, *Essentials of Robust Control*, Prentice-Hall.